

Clinical Study on Using Thermal Texture Maps in SARS Diagnosis

Wei Wang, Yi Zeng, Daqing Ma, Zhengyu Jin, Hao Wu, Chunwang Yuan, Yun-er Yuan,
Zhongqi Liu, Chen Wang, Hairong Qi,

Abstract—This paper helps define infrared (IR) imaging as a complementary tool to high-speed computer tomography (CT) in the diagnosis of severe acute respiratory syndrome (SARS). We refer to the images captured from IR imaging as thermal texture maps (TTM). Although IR imaging has been criticized of generating high false alarm rate for the lack of quantitative measurement on the size, depth, and shape information of the tumor, we present a new methodology that reveals the depth information and the activity of tumor from processing the surface temperature. The derivation is obtained without solving the ill-posed inverse heat transfer problem. We evaluate the clinical value of TTM in SARS diagnosis and compare the performance with CT. The study took place at Beijing You An Hospital, Beijing, P. R. China. It was conducted on a group of 111 confirmed SARS patients between March 10, 2003 and June 18, 2003. Both CT and TTM are used on the same patient in diagnosis and monitoring. We conclude that TTM is able to depict the position, morphology, and progress of lesions with the same degree of success as CT. The combination of CT and TTM can improve the quality and accuracy of SARS diagnosis.

Index Terms—Severe acute respiratory syndrome (SARS), Infrared (IR) imaging, Thermal Texture Map (TTM), Computer Tomography (CT).

I. INTRODUCTION

SEVERE acute respiratory syndrome (SARS) is a viral respiratory illness caused by a coronavirus, called SARS-associated coronavirus (SARS-CoV). Its first outbreak was recorded in Guang Dong Province of southern China in November 2002. In just a few months, the disease spread to

Wei Wang and Chunwang Yuan are with the Department of Radiology, Beijing You An Hospital, Beijing, P. R. China.

Hao Wu is with the Department of infection, Beijing You An Hospital, Beijing, P. R. China.

Yi Zeng is with Central Disease Control of China

Daqing Ma is with the Department of Radiology, Beijing You An Hospital, Beijing, P. R. China.

Zhengyu Jin is with the Department of Radiology, Beijing Xie He Hospital, Beijing, P. R. China.

Yun-er Yuan is with Institute of Basic Medical Science, China Army General Hospital, Beijing, China

Zhongqi Liu and Chen Wang are with China People Health Association, Beijing, P. R. China.

Hairong Qi is with the University of Tennessee, Knoxville, TN 37996 (corresponding author is Hairong Qi, phone: 865-974-8527, fax: 865-974-5483, email: hqi@utk.edu)

28 countries around the world. According to the World Health Organization (WHO) [1], during the SARS outbreak of 2003, a total of 8,098 people worldwide became sick with SARS; of these, 774 died. This high infection rate and high fatality rate (1 out of 10.5 infected) are largely due to the limited understanding to the disease.

Scientists around the world have been trying to decode the genetic sequence of SARS in the hope of developing SARS antibody. However, till now, the most effective treatment still relies on good, intensive, and supportive care. Under this circumstance, early detection, early diagnosis, and immediate isolation are the keys to preventing another outbreak of SARS. Active image monitoring and analysis of the full clinical stages of illness are important for accurate diagnosis and treatment. Today, the standard diagnostic procedures are based on chest X-ray radiology exams and Computer Tomography (CT).

In order to improve the process of diagnosing and monitoring SARS, a study has taken place in China that evaluates the clinical value of *infrared imaging* (IR) in the diagnosis of SARS. We use the term *thermal texture maps* (TTM) to represent the images captured from IR imaging.

IR imaging is a physiological test that measures the physiology of the blood flow and behavior of the nervous system by means of precise temperature measurement. Unlike imaging techniques such as X-ray radiology and CT that primarily provide information on the anatomical structures, IR imaging provides functional information not easily measured by other methods [5]. Compared to other imaging modalities, IR imaging is non-invasive, non-ionizing, risk-free, patient-friendly, and inexpensive. It has the potential to provide more dynamic information of the patho-physiological abnormalities occurring in the human body at an early stage of disease development since the disease can affect a small area but can be fast growing making it appear as a high temperature spot in the TTM. However, this provides only a surface image which can be read principally by a qualitative technique that may not reveal quantitative information of the potential tumor. In this paper, we present a new methodology which can estimate the depth information of lesion through surface temperature slicing. We evaluate the clinical value of IR imaging as a complementary tool to CT in SARS diagnosis.

Our study is conducted on a group of 111 patients that have been pre-confirmed to be SARS patients by both clinical and

laboratory diagnosis. Two imaging modalities, CT and IR, are used on each patient. The diagnostic results are cross-compared in order to study the clinical value of IR in the detection and monitoring of SARS.

The outline of the paper is as follows: Sec. II briefly summarizes the pathology of SARS. Sec. III describes the principles of using IR imaging in monitoring the metabolic activity of human body. Sec. IV discusses how IR imaging can be used to assist the diagnosis and monitoring of SARS. Sec. V describes the design of clinical study in detail. And Sec. VI performs a comprehensive analysis and evaluation on the results obtained from both CT and TTM.

II. THE PATHOLOGY OF SARS

Several studies have been conducted since SARS outbreak to help understand the pathology of SARS [7], which includes both parenchymal and interstitial abnormalities. Here, we divide the SARS infection process into three stages, interstitial infiltration, duplication, and macrophage increment.

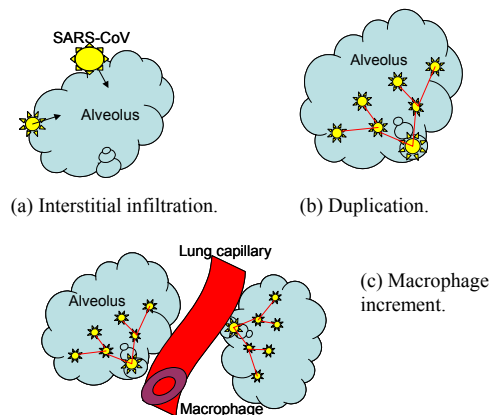


Figure 1. SARS-CoV infection stages.

In the early stage of SARS, the virus were mainly interstitial infiltrative as shown in Figure 1(a). After penetrating into the alveoli, the SARS-CoV starts to duplicate itself in massive amount [Figure 1(b)] which eventually triggers the human immune system to react, causing proliferation of macrophages that could damage or block lung capillary, shown in Figure 1(c).

In the following sections, we show how IR imaging can detect and monitor this abnormal metabolic activity of human body triggered by the invasion of SARS-CoV from different perspectives.

III. THERMAL TEXTURE MAPS IN MONITORING HUMAN BODY METABOLIC ACTIVITIES

IR imaging has been applied to a wide spectra of applications, ranging from the military, industrial engineering, to modern medicine. It is non-invasive, non-ionizing, risk-free, patient-friendly, and inexpensive, which makes it a valuable tool to assist diagnosis.

IR radiation occupies the region on the electromagnetic spectrum between visible and microwaves. All objects in the universe emit radiations in the IR region as a function of their temperature. As an object gets hotter, it gives off more intense infrared radiation, and it radiates at a shorter wavelength [5].

Temperature is a long established indicator of health. Before Galileo invented thermoscope, the ancient Egyptians used fingers as scanners to monitor the surface temperature of the human body [2]. Human eye cannot detect IR rays, but they can be detected using the thermal infrared cameras and detectors.

A. Principles of IR Imaging

All objects at temperature above absolute zero emit electromagnetic radiation spontaneously, called the *natural thermal radiation* [5]. The heat emanating on to the surface from the infected tissue and the surrounding blood flow can be quantified using the Pennes [8] bio-heat equation. This equation includes the heat transfer due to conduction through the tissue, the volumetric metabolic heat generation of the tissue, and the volumetric blood perfusion rate whose strength is considered to be the arterio-venous temperature difference. The equation is given as:

$$k\Delta^2 T - c_b w_b (T - T_a) + q_m = 0$$

where k is conductivity, q_m is volumetric metabolic rate of the tissue, $c_b w_b$ is the product of the specific heat capacity, the mass flow rate of blood per unit volume of tissue T is the unknown tissue temperature, and T_a is the arterial temperature.

In theory, given the heat emanating from the surface of the body measured by IR imaging, by solving the inverse heat transfer problem, we can obtain the heat pattern of various internal elements of the body. Different methods of solving the bio-heat transfer equation have been presented in literature [3][4]. Although it is possible to calculate the thermal radiation from a thermal body by thermodynamics, the complexity of the boundary conditions associated with the biological body makes this approach impractical.

B. The Thermal-Electric Analog

As the living cells within a biological body are constantly undergoing metabolic activities, the biochemical and the physical metabolic processes generate heat. Thus the amount of radiation on the surface of the human body can reflect its metabolic rate. The theory underlying conventional thermographic techniques as applied to cancer is that the change of the pulse distribution around a cancerous area and the rate of metabolism are greater than the general tissue, resulting in a higher temperature at the skin surface [6].

Even though the temperature of the skin surface can be measured, if the relationship between the surface temperature and the emissions from inside of the body cannot be established, the application of IR imaging technique is still limited. Pennes' bio-heat equation models the process of heat transfer but has its limits in practice. Thus, a new method that

does not require a direct solution to the inverse heat transfer problem, the thermal-electric analog, comes into light.

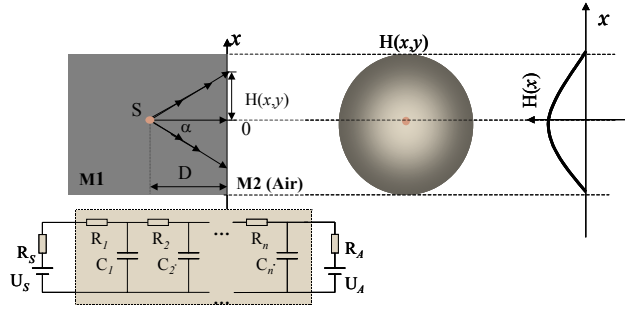


Figure 2. The thermal-electric analog.

Figure 2 illustrates the analogy between thermodynamics systems and the electrical circuit, where the heat source S inside the human body can be simulated as a battery with voltage U_S , the heat loss inside the heat source can be simulated as the heat loss on a resistor R_S . The temperature of the heat source can then correspond to the voltage of the battery, and the heat current to the circuit current. Similarly, we can map the heat source in the air (outside the human body) as U_A , and the heat loss as R_A . The set of R_i 's and C_i 's correspond to the unit heat resistance and heat capacity along each radiation line.

The circuit in Figure 2 only shows the analogy for one radiation line. In the study of breast cancer, it is reasonable to assume that the medium between the heat source (S) and the surface is homogeneous. Therefore, the radiation pattern sensed by the IR camera at the surface should have a distribution like Gaussian as shown in Figure 2. The surface temperature $H(x)$ corresponds to the output voltage can then be calculated,

$$H(x) = U_S - \frac{\sum_{i=1}^n R_i}{R_S + R_A + \sum_{i=1}^n R_i} \times (U_S - U_A)$$

and

$$n = \left\lfloor \frac{D}{R_0 \cos \alpha} \right\rfloor,$$

where $\lfloor a \rfloor$ represents the largest integer less than a , n is the number of resistors used in the circuit, D is the depth of the heat source, and R_0 is the unit heat loss in a certain medium (or the heat resistance rate). Different parts of human body have different heat resistance rate, as shown in the following table,

Body parts	Heat resistance rate
Fatty tissue	0.1 ~ 0.15 ⁰ C/cm

Muscle	0.2 ⁰ C/cm
Bone	0.3 ~ 0.6 ⁰ C/cm

The thermal-electric analog provides a convenient way to estimate the depth of the heat source.

C. Estimation of the Depth of the Heat Source

The depth estimation is based on the assumption that we can use Gaussian to model the distribution of the surface temperature.

Half power point is a useful property of Gaussian distribution. The property says that the half power point divides the area enclosed by the Gaussian into equally half. If we slice the Gaussian from top to bottom at a fixed interval as shown in Figure 3, the increment of the radius in the horizontal direction would not have dramatic change until the half power point is crossed. From Figure 3, we can see that the relative increment of the radius between the first slice and the second slice is 34 pixels, and 40 pixels between the second slice and the third slice, but 116 pixels between the third slice and the fourth slice. Therefore, the half power point is at the position of the third slice.

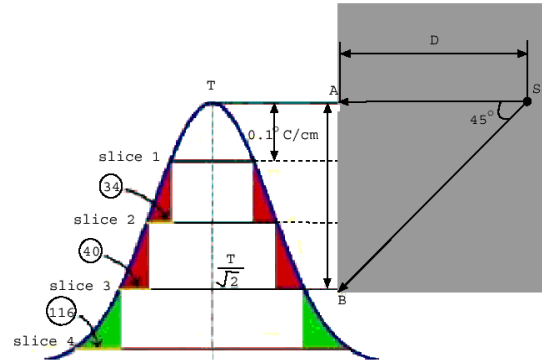


Figure 3. Illustration of half power point of Gaussian and the depth of the heat source.

Suppose the temperature of the heat source is H_0 . In the right triangle formed by SAB , the hypotenuse (SB) is equal to H_0 and the sides ($SA = AB$) should be equal to $0.707 H_0$. The horizontal side (SA) is the depth of the heat source, and the vertical side (AB) is the temperature drop between the maximum value of the Gaussian and the half power point. In another work, if we can find the half power point, we can find the depth of the heat source.

Each slice of the Gaussian curve corresponds to a temperature deduction of 0.1 degree. For the application of SARS diagnosis, based on the heat resistance rate of fat tissues, the 0.1 degree temperature drop corresponds to a distance of 1cm. Therefore, by slicing (decreasing) the surface temperature at a certain degree per step, we can find the half power point with the accuracy at the level of centimeter.

IV. SARS DIAGNOSIS PRINCIPLES USING CT AND TTM

It is considered, in general, that CT indications of SARS are in the density, appearance and distribution of lesions. Density can show ground-glass opacity and/or consolidation. The shape of lesion could be focal, multi-focal, nodular, patchy, segmental, lobar and in extensive conglomerated lesions. In addition, the lesions appear mostly in the lower lung areas and sub-pleural regions.

On the other hand, the TTM indications of SARS are in the discovery of abnormal heat patterns. This, combined with the depth estimation methodology discussed in Sec. III, can be used to assist SARS diagnosis. A study of the human cardiovascular system shows a couple of blood vessel concentration areas, among which the place where the jugular veins, carotid arteries, subclavian artery/vein meet is one of the most concentrated, and correspondingly, the hottest. We refer to this area as subclavian area. Therefore, when slicing the TTM of a normal patient, the subclavian area should first appear as white since it has a higher temperature than other parts of the human body. Otherwise, some abnormal metabolic activities must exist. Figure 4 shows the slicing results of the TTM of a normal patient. We observe that both the left and right subclavian areas appear as white earlier than the lung area. This rule of thumb applies to regular lung diseases as well. Figure 5 shows the slicing results of the TTM of a patient with lung TB condition. We can see that in the slicing process, the subclavian area is still the first one that goes white (the hottest).

Figures 5 and 6 show the slicing results of TTMs from two SARS patients. In both cases, we observe that the subclavian areas do not show as white until the slicing causes portions of the lung area to be white. This indicates some serious abnormalities in the metabolic activity of the lung, which through clinical study, has been identified as one of the symptoms in the diagnosis of SARS.

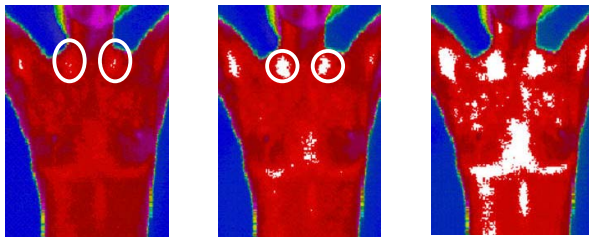


Figure 4. TTM slicing of normal case.

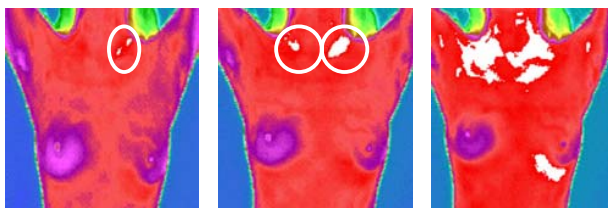


Figure 5. TTM slicing of lung TB condition.

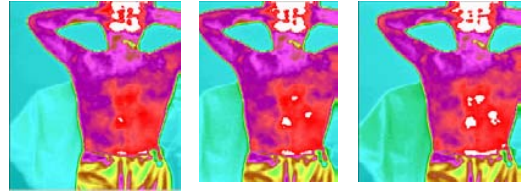


Figure 5. TTM slicing of SARS patient 1.

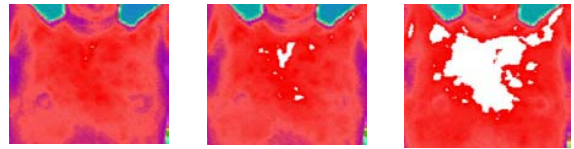


Figure 6. TTM slicing of SARS patient 2.

At the initial and progress stages of SARS development, there is an increase in the thermal radiation of the lesions, and solid density heat structures normally appear over 3cm deep from the surface of the skin that corresponds to the lesions found in CT.

In the later stages, the SARS patient may develop adult respiratory distress syndrome (ARDS), in which the main pathological abnormality is pulmonary edema. TTM would show the appearance of low thermal radiation zones and solid heat structures in lung areas, along with possible metabolic changes in the other organs.

At the recovery stage, there is normally decreased thermal radiation, with “cool zone” structures or “oval cold” solitary density structures that match lesions that display interstitial hyperplasia and compensatory emphysema, or cavities with purulence in the CT. TTM also shows decreased thermal radiation of the spleen, and increased thermal radiation of the spine.

V. STUDY DESIGN

The study is conducted between March 10, 2003 and June 18, 2003 on 111 SARS patients (pre-confirmed by both clinical and laboratory diagnosis) at Department of Communicable Diseases of Beijing You An Hospital, Beijing, China. All cases met the standard SARS diagnosis criteria set by the China Ministry of Health and the United States Center for Disease Control and Prevention (CDC). Among the 111 examined patients, 54 were male (24 cases between 12-30 years of age, 30 cases between 31-62 years of age, the average

age being 34) and 57 were female (22 cases between 14-30 years of age, 35 cases between 31-68 years of age, the average age being 36). Out of the 111 cases, 98 claimed to have had close contact with another SARS patient or patients; their symptoms included fever (94.4%), nonproductive cough (92.7%), chest pain (83.3%), headache (55.6%) and Diarrhea (3%). Among the 111 patients, only 3 experienced no major symptoms. Laboratory tests of all the patients showed the following common symptoms: a) White blood cell count and lymphocyte count decreased during the earlier phases of the disease; b) CD3, CD4, and CD8 T-cell counts were decreased - CD4 decreased most severely. T-cell counts were at their lowest 10-14 days after the symptoms started. The lower the T-cell count, the greater the severity of the SARS disease.

CT was performed for every patient upon admission into the hospital. Regular follow-up examinations were performed afterwards once every 4 to 6 days for a total of 80 to 90 days. TTM examinations were performed between May 19 and June 18, 2003 for all 111 cases. The CT was performed with a High-speed DX/I helical CT (HRCT) unit manufactured by GE Company with slice thickness and slice interval of 10 mm from lung apices to phrenic angles. The HRCT was performed with a 140 kV, 180mA, with a slice thickness of 2 mm, and slice interval of 2 to 4 mm and bone algorithm reconstruction. The TTM examinations were performed in three positions; anterior, dorsal, and right lateral of body with a TSI-21M system manufactured by Bioyear Group Inc. More than 3 senior radiologists and scientists assessed and reviewed all images.

VI. RESULT ANALYSIS AND PERFORMANCE COMPARISON

From the clinical study, we summarize our findings in the following three subsections.

A. Image Characterization of the Initial Stage of SARS

Small focal or multiple and extensive patches of infiltration density showed in 28 out of 111 cases, and among those 28, small focal opacity were more common (24/28, 85.7%). HRCT could show the lesion more clearly. It indicated that the focal ground glass opacity was common. TTM depicted abnormally increased thermal radiation and solitary density structures that correspond to lesions displayed in the HRCT, as well as an abnormal thermal radiation increase in the spleen and a decrease in the spine.

B. Imaging Characterization of the Progressive Stage of SARS

In this stage of SARS development, we found that 1) the uniform ground-glass-like density with ill-defined border and blood vessels (throughout the whole course of the continued follow-up observation) showed in 18 cases of 111 (16.2%), 2) the mainly ground-glass-like density with consolidation showed in 85 cases of 111 (76.6%), and 3) the mainly consolidation density with air-bronchogram image showed in 8 cases of 111 (7.2%).

Again, TTM dynamic manifestation depicted abnormally increased thermal radiation as well as solitary density structures that correspond to lesions displayed in the CT. The abnormal thermal radiation reached its highest level in the spleen. TTM also shows abnormality in the functions of other organs caused by SARS, or possibly by other, related or unrelated diseases.

C. Image Characterization of the Recovery Stage of SARS

In the *recovery stage* of SARS development, most of the patients exhibited normal images. 4 of the 111 cases showed pulmonary interstitial hyperplasia with multiple linear, reticular or honey-combed patterns. Some also displayed an increase in density of the subpleural arc line and thickened interlobular septa, or compensatory emphysema and reduced thoracic cage. 5 of the 111 cases showed focal or multi-cavity with purulence. TTM manifestations depicted abnormally low thermal radiation with "cool zone" structures that corresponded to lesions that displayed interstitial hyperplasia or compensatory emphysema, or "oval cold" solitary density structures that corresponded to cavities with purulent in the CT and radiograph. TTM continued to show a decrease in thermal radiation of the spleen and an increase in the thermal radiation of the spine.

D. Dynamic Evolution Imaging in SARS

Dynamic follow-up observations of changes in the images of SARS patients are indispensable, which is normally not necessary in other pneumonias. Imaging changes in SARS patients are not only dependent on the inherent development of the disease itself, but also on treatment management, treatment effects, age, previous health, etc. Among the 111 cases, some of the small patchy densities in the early stages progressed into extensive lesions in a very short time – roughly 24 to 48 hours. Such dynamic change was largely consistent with worsening of the clinical condition. Diffusely scattered lesions in both lungs are suggestive of early ARDS. Progression from focal ground-glass-like density to extensive density with consolidation (CT) and appearance of low thermal radiation zone with abnormal solid density structure of heat (TTM) and signs of rapid development of the lesion are compatible with the clinical features of ARDS.

The decreased opacity showed resolution of the lesion, and eventual disappearance of low thermal radiation zone, along with decreased density of lesion structures and increased appearance of spine line and liver heat.

During the recovery stage, some patients displayed complicated pulmonary interstitial fibrosis or multiple abscess-like cavities. HRCT showed linear, reticular and honey-comb-like densities. Radiographs cannot demonstrate detailed interstitial changes. Radiographic changes of lung markings are nonspecific for interstitial fibrosis. The low thermal radiation zone of TTM suggests the possibility of interstitial fibrosis.

VII. COMPARISON OF THE USAGE OF CT AND TTM IN SARS DIAGNOSIS

HRCT may demonstrate subtle focal lesions in the early stage of SARS, especially ground-glass-like density; corresponding TTM images may show solid density structures of lesions as well as other functional image information related with illness.

Figure 7 shows a side-by-side comparison of using TTM and CT in SARS diagnosis. The TTM slicing shows the abnormal heat pattern with the depth of heat source 6cm from skin surface. In addition, the subclavian area has a lower temperature than that of the right lung since the lower part of the right lung becomes white first. The CT image of April 26, 2003 showed the right lung lesion of SARS in its progress stage. The CT image of May 23, 2003 showed right lung lesion of SARS in its recovery stage. TTM image of May 23, 2003 indicates the abnormal heat pattern of lower right lung lesion which is confirmed by the CT image of the same date.

During the treatment of SARS, it is necessary to monitor the chest condition, such as the distribution and extent of the lesion and the effect of treatment. Following the initial stage of the disease, TTM could become the main imaging modality of examination of SARS since it can show the general manifestation of the disease. In addition, it is convenient, less expensive, and requires less exposure to potentially harmful radiation. During the recovery stage, if there is any change towards possible pulmonary interstitial hyperplasia, HRCT and TTM should be used to reveal the details of the interstitial and functional low-thermal radiation zone. The different features of these two imaging modalities are summarized in the following table.

	CT	TTM
Radiation	Yes	No
Protection	Difficult	Easy
Exam Time	25 minutes	5 minutes
Cost	High	Low
Environment Risk	Yes	No
Mobility	Worst	Best
Consumption	30KW	0.3KW

TTM, as a functional imaging modality, is able to quickly examine and assess the position, morphology, and progress of SARS lesions, in the meantime effectively monitoring treatment and patient recovery by providing information regarding the functional condition of the liver, spleen, kidney and other organs.

TTM can be used as first line imaging system for SARS screening, followed by CT and TTM to carry out further differential diagnosis, including full-course treatment monitoring. This combination of the two imaging systems should be the most beneficial for future prevention and treatment of SARS.

ACKNOWLEDGMENTS

The authors are grateful to colleagues for the very instructive suggestions which led to the much improved quality of the paper: Dr. N. Patronas, Dr. A. H. Gandjakhche, and Dr. M. Hassan from National Institute of Health (NIH), Dr. R. Xue from Johns Hopkins Medical Center, Dr. J. Head from the Mastology Institute in Baton Rouge, LA, Mary Diakides and Dr. Nicholas Diakides from Advanced Concept Analysis, Inc.

REFERENCES

- [1] <http://www.niaid.nih.gov/factsheets/sars.htm>
- [2] <http://www.thermology.com/history.htm>
- [3] C. L. Chan, "Boundary element method analysis for the bioheat transfer equation," in *ASME J. Heat Transfer*, vol. 114, pp. 358-365, 1992.
- [4] T. R. Hsu, N. S. Sun, G. G. Chen, "Finite element formulation for two dimensional inverse heat conduction analysis," in *ASME J. Heat Transfer*, vol. 114, pp. 553-557, 1992.
- [5] B. F. Jones, "A reappraisal of the use of infrared thermal image analysis in medicine," in *IEEE Transaction on Medical Imaging*, vol. 17, no. 6, pp. 1019-1027, December 1998.
- [6] Z. Liu, C. Wang, "Method and apparatus for thermal radiation imaging," United States Patent No.: 6,023,637, 2000.
- [7] J. M. Nicholls, L. L. Poon, K. C. Lee, W. F. Ng, S. T. Lai, *et al.*, "Lung pathology of fatal severe acute respiratory syndrome," in *Lancet*, vol. 361, no. 9371, pp. 1773-1778, May 24, 2003.
- [8] H. H. Pennes, "Analysis of tissue and arterial blood temperature in resting human forearm," in *Journal of Applied Physiology*, vol. 2, pp. 93-122, 1948.

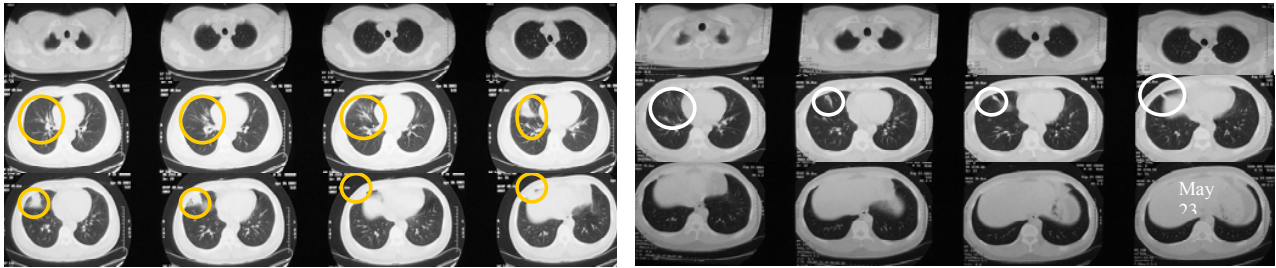


Figure 7. Comparison between CT and TTM in SARS diagnosis – TTM image of May 23, 2003 indicates the abnormal heat pattern of lower right lung lesion which is confirmed by the CT image of the same date. First row: TTM slicing shows the abnormal heat pattern with the depth of heat source 6cm from skin surface; in addition, the subclavian area has a lower temperature than that of the right lung. Second row: (left) CT image of April 26, 2003 showed right lung lesion of SARS progress stage; (right) CT image of May 23, 2003 showed right lung lesion of SARS recovery stage.